SUPPORTING INFORMATION

Synthesis of and iodine capture with MS_x (Ag_2S, Bi_2S_3, Cu_2S)-polyacrylonitrile composites

Brian J Riley[a1], Saehwa Chong [a] , and Nathan L. Canfield

[a] *Pacific Northwest National Laboratory, 902 Battelle Blvd, Richland, WA 99354.*

Keywords: iodine sorbent; radioiodine, silver sulfide; bismuth sulfide; copper sulfide; polyacrylonitrile

[1] Corresponding author: brian.riley@pnnl.gov; +1 (509) 372-4651

1 Conceptual Design of Sorbent System

The conceptual design for the current study is shown in Figure S1. The loading temperature of 130°C was selected for a few reasons. In previous studies,[S1, 2] temperatures in this range worked well for loading PAN composites. Higher temperatures (e.g., 150°C) showed evidence of iodine interactions with the PAN matrix itself,[S3] while studies at room temperature showed very little PAN-iodine interactions.[S4] Thus, it seems that 130°C is in a range of relevant temperature for iodine off-gas capture from radiological process implementation and in the sweet-spot for loading onto an active getter with minimal loading into the PAN. Also, the loading times selected for this study were based off our previous work.[S1] While the reactions shown in Figure 1 (in the paper) predict the formation of elemental sulfur with a melting temperature of 112.8°C, it is more than likely that conversion of the metal sulfides (i.e., Ag_2S, Bi_2S_3, and Cu_2S) into metal iodides (i.e., AgI, BiI_3, CuI) will result in the formation of elemental sulfur that will melt within the sorbent. While it is possible that these will agglomerate and could clog the internal pores of the PAN scaffold, this was not generally observed in SEM-EDS analyses of iodine-loaded MS_x-PAN composites in this study except for the 80Cu_2S-PAN+I sample (see Figure 4 in the paper).

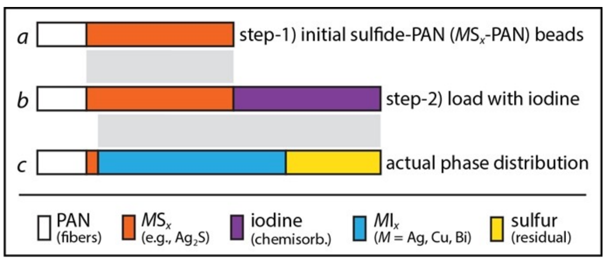

Figure S1. Graphic representation of multi-phase sorbent after iodine reaction showing (a) the initial MS_x-PAN composite, (b) the MS_x-PAN composite after iodine loading, and (c) the actual phase distribution of (b) according to the thermodynamic predictions; note that these values are arbitrarily shown as an example.

The first step in this study was to make PAN composites with Ag_2S, which is why different loadings were used (i.e., 75%, 80%, and 90%). The overall appearance of the 90Ag_2S-PAN composites showed that the spherical-type shapes were not maintained as well at loadings higher than 80 mass% so the 80 mass% loading level was used for the subsequent samples produced, i.e., 80Bi_2S_3-PAN and 80Cu_2S-PAN.

2 Making Composites

Table S1. Compositions for each batch of MS_x-PAN composite beads including the sample ID, mass of MS_x (m_{MS_x}), mass of PAN (m_{PAN}), and the volume of DMSO (V_{DMSO}).

Sample	m_{MS_x} (g)	m_{PAN} (g)	V_{DMSO} (mL)
75Ag_2S-PAN	0.6015	0.2014	3.0
80Ag_2S-PAN	0.8003	0.2004	3.0
90Ag_2S-PAN	1.2004	0.1336	2.0
80Bi_2S_3-PAN	0.8004	0.2002	3.0
80Cu_2S-PAN	0.8009	0.2004	3.0

3 X-Ray Diffraction Data

Table S2. Summary of XRD data for as-received MS_x reagents including the Inorganic Crystal Structure Database (ICSD) number, space group (SG), SG#, mass% of the phase based on Rietveld refinements, and the goodness of fit (Rwp) value.

Sample ID	Phase	ICSD#	Space Group	SG#	Mass%	Rwp
Ag_2S powder	Ag_2S	182916	$P2_1/c$	14	100.0	4.320
Bi_2S_3 powder	Bi_2S_3	153946	*Pnma*	62	100.0	14.772
Cu_2S powder	Cu_2S	–	*Abm*2	39	100.0	–

Table S3. Summary of XRD data for as-made MS_x-PAN composites including the ICSD number, space group (SG), SG#, mass% of the phase based on Rietveld refinements, and the Rwp value.

Sample ID	Phase	ICSD#	Space Group	SG#	Mass%	Rwp
75%Ag_2S-PAN	Ag_2S	182916	$P2_1/c$	14	100.0	4.504
80%Ag_2S-PAN	Ag_2S	182916	$P2_1/c$	14	100.0	4.435
90%Ag_2S-PAN	Ag_2S	182916	$P2_1/c$	14	100.0	4.725
80%Bi_2S_3-PAN	Bi_2S_3	153946	*Pnma*	62	100.0	8.144
80%Cu_2S-PAN	Cu_2S	100333	*Abm*2	39	100.0	–

Table S4. Summary of XRD data for iodine-loaded MS_x-PAN composites including the ICSD number, space group (SG), SG#, mass% of the phase based on Rietveld refinements, and the Rwp value.

Sample ID	Phase	ICSD#	Space Group	SG#	Mass%	Rwp
75%Ag_2S-PAN +I	γ-AgI	52361	*F*-43*m*	216	70.8	5.568
	β-AgI	15589	$P6_3mc$	186	29.2	
80%Ag_2S-PAN+I	γ-AgI	52361	*F*-43*m*	216	86.2	4.490
	β-AgI	15589	$P6_3mc$	186	13.8	
90%Ag_2S-PAN+I	γ-AgI	52361	*F*-43*m*	216	81.9	5.095
	β-AgI	15589	$P6_3mc$	186	18.1	
80%Bi_2S_3-PAN+I	BiI_3	36182	R-3	148	100.0	6.475
80%Cu_2S-PAN+I	CuI	163427	*F*-43*m*	216	100.0	5.374

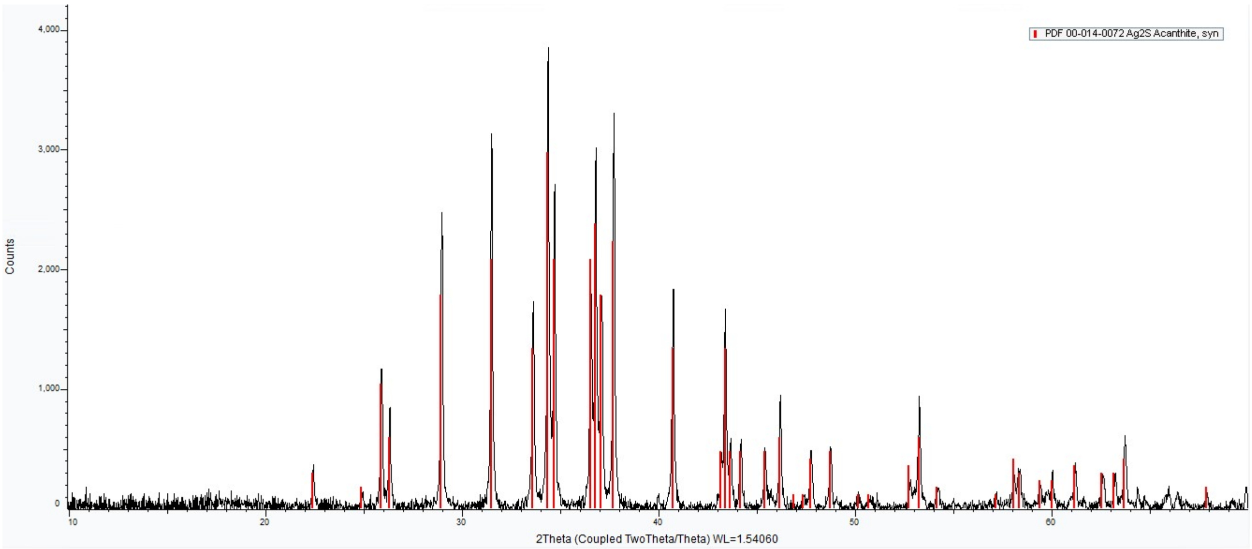

Figure S2. As-received Ag_2S reagent showing ICDD peak location fitting with the Ag_2S (acanthite, syn) phase (PDF 14-0072).

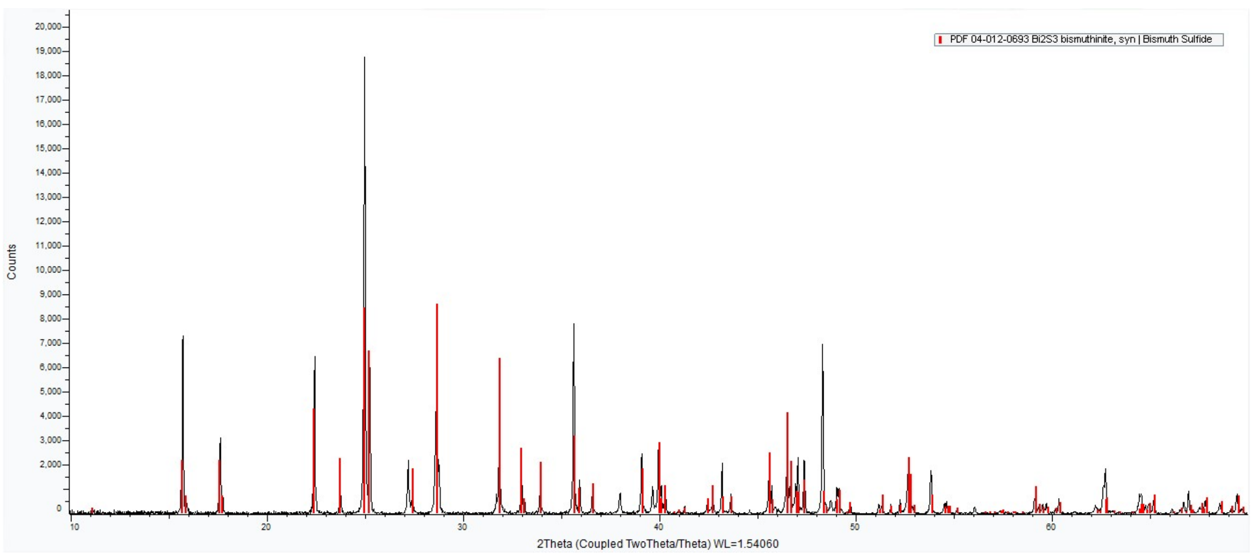

Figure S3. As-received Bi_2S_3 reagent showing ICDD peak location fitting with the Bi_2S_3 (bismuthinite, syn) phase (PDF 04-012-0693).

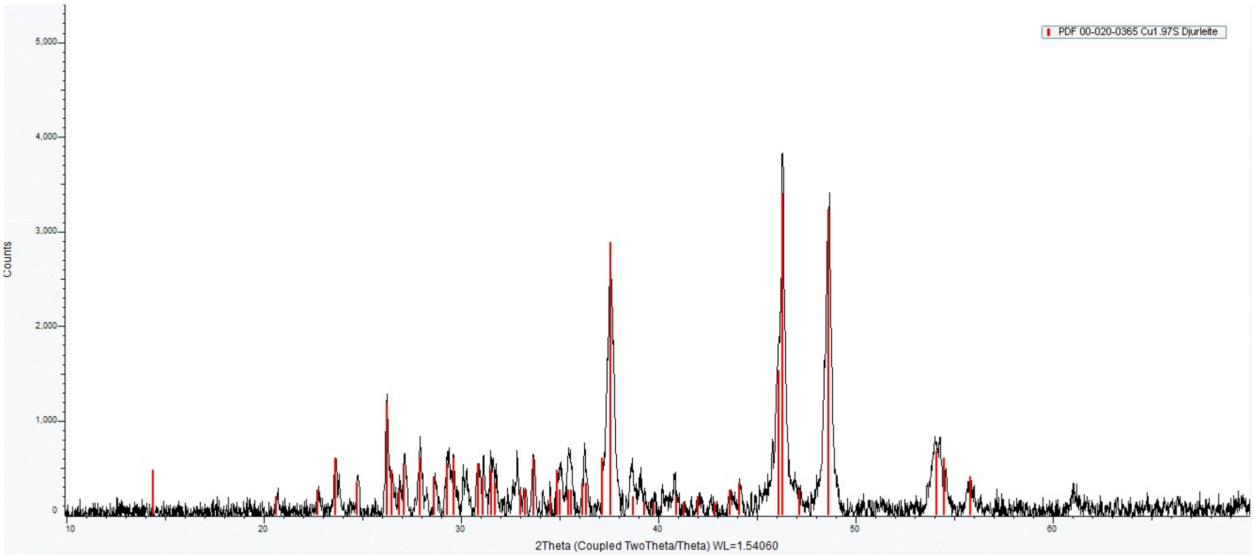

Figure S4. As-received Cu_2S reagent showing ICDD peak location fitting with the $Cu_{1.97}S$ phase (20-0365) not in the ICSD.

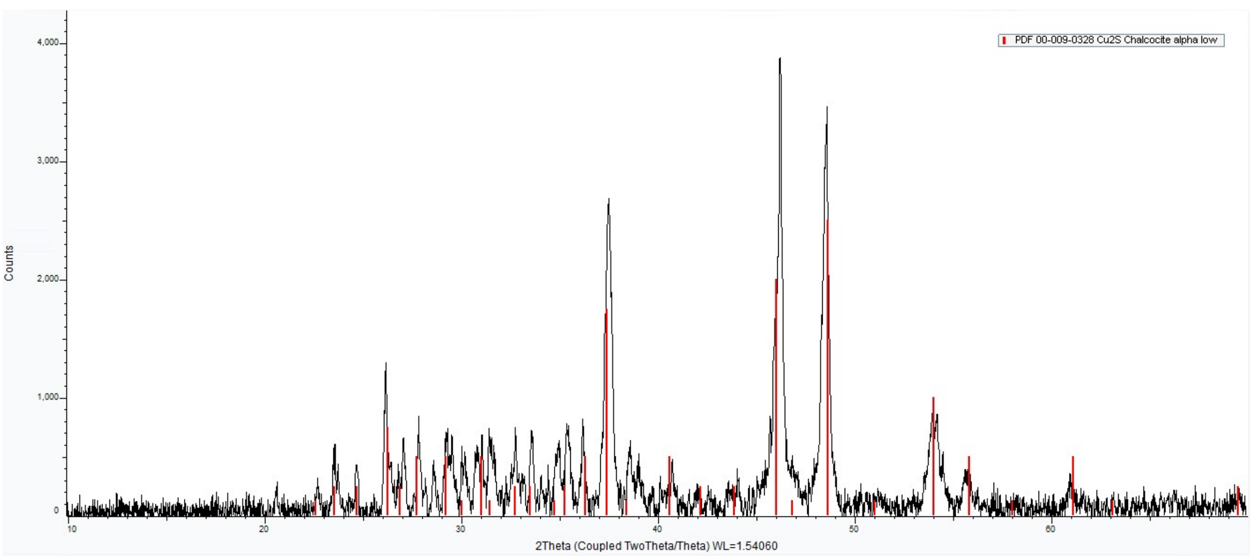

Figure S5. As-received Cu_2S reagent showing ICDD peak location fitting with the Cu_2S phase (09-0328) not in the ICSD.

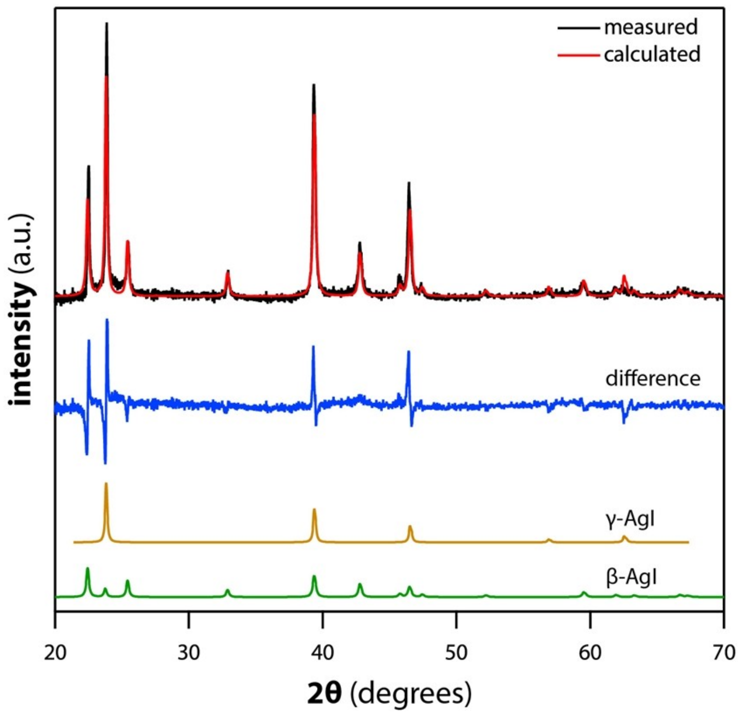

Figure S6. Summary of Rietveld refinement for 75%Ag_2S-PAN+I showing the peak contributions for γ-AgI and β-AgI.

4 Scanning Electron Microscopy and Energy Dispersive Spectroscopy Data

EDS was collected in low vacuum conditions (30Pa). Due to the partial atmosphere in the chamber, the electron beam will be scattered. Therefore, any quantitative results are for comparison only, and are not truly quantitative.

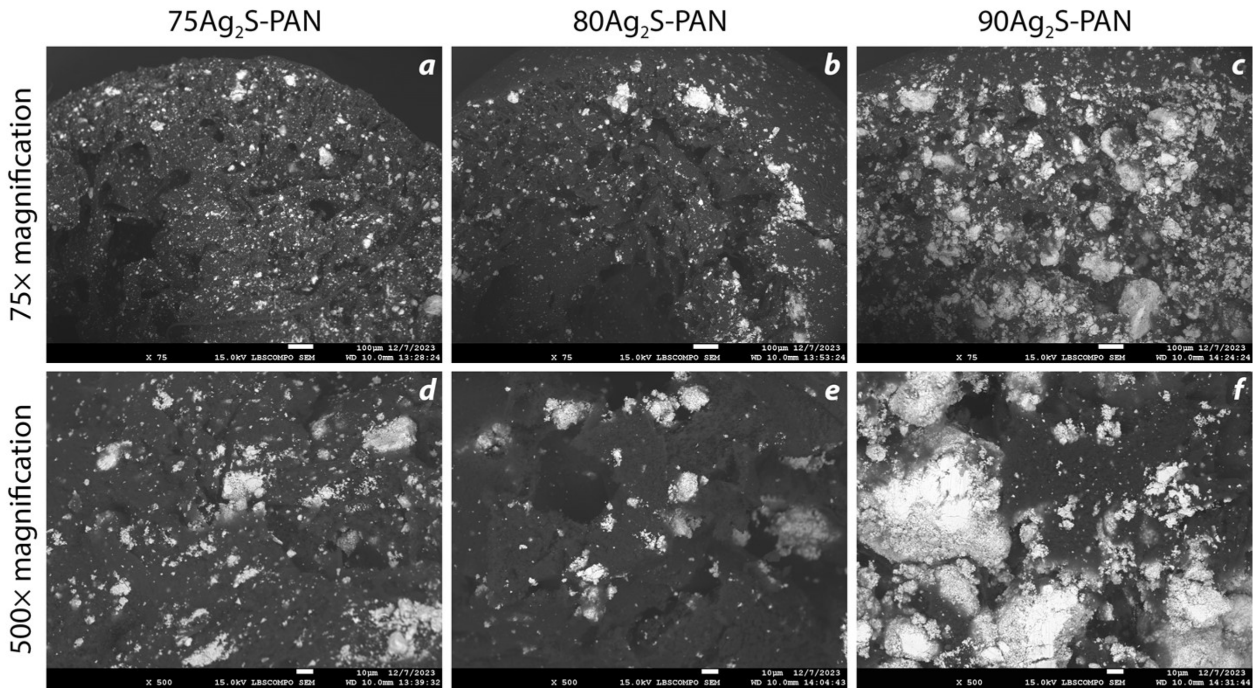

Figure S7. SEM micrographs for Ag_2S-PAN samples without iodine including (a-c) 75× and (d-f) 500× magnification micrographs for (a,d) 75Ag_2S-PAN, (b,e) 80Ag_2S-PAN, and (c,f) 90Ag_2S-PAN.

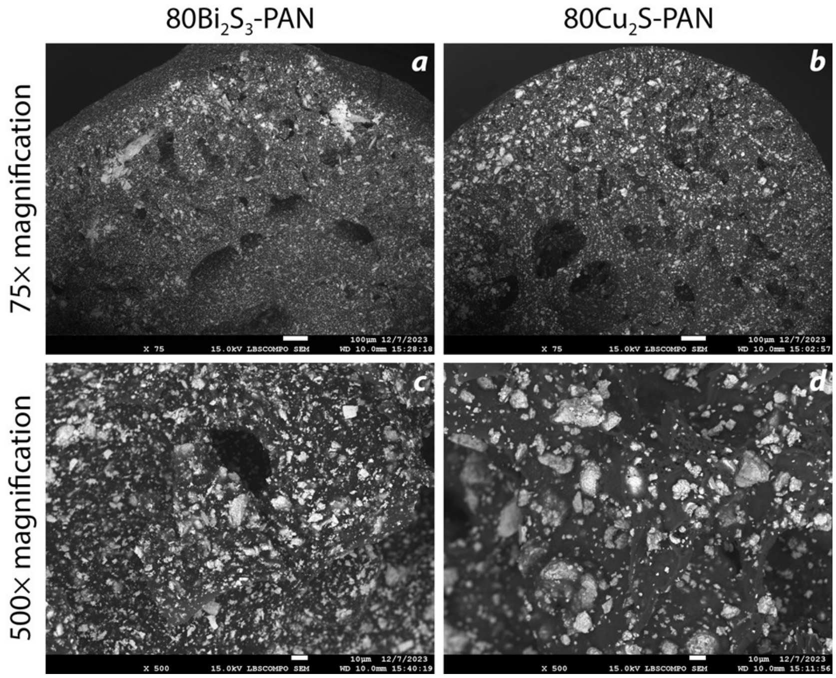

Figure S8. SEM micrographs for (a,b) 80Bi_2S_3-PAN and (c,d) 80Cu_2S-PAN without iodine including (a,b) 75× and (c,d) 500× magnification micrographs.

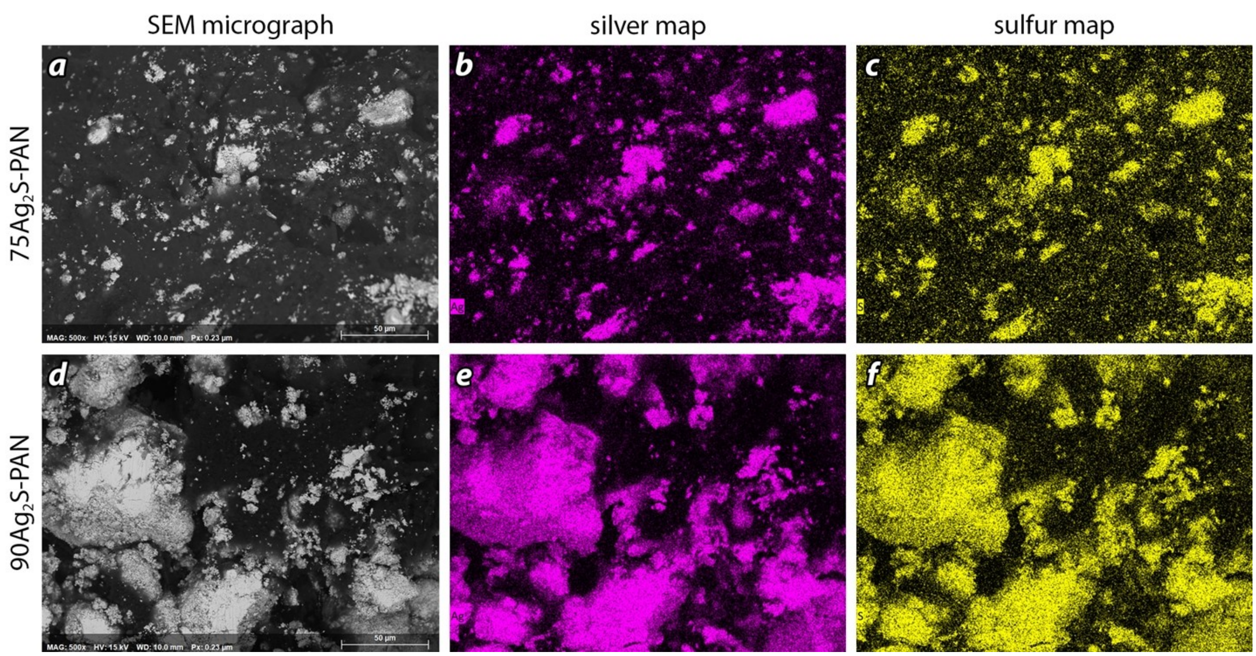

Figure S9. (a,d) SEM and (b,c,e,f) EDS data for (a-c) 75Ag_2S-PAN and (d-f) 90Ag_2S-PAN composites showing the (b,e) Ag-maps and (c,f) S-maps. Note that the 80Ag_2S-PAN data is not provided but looked similar.

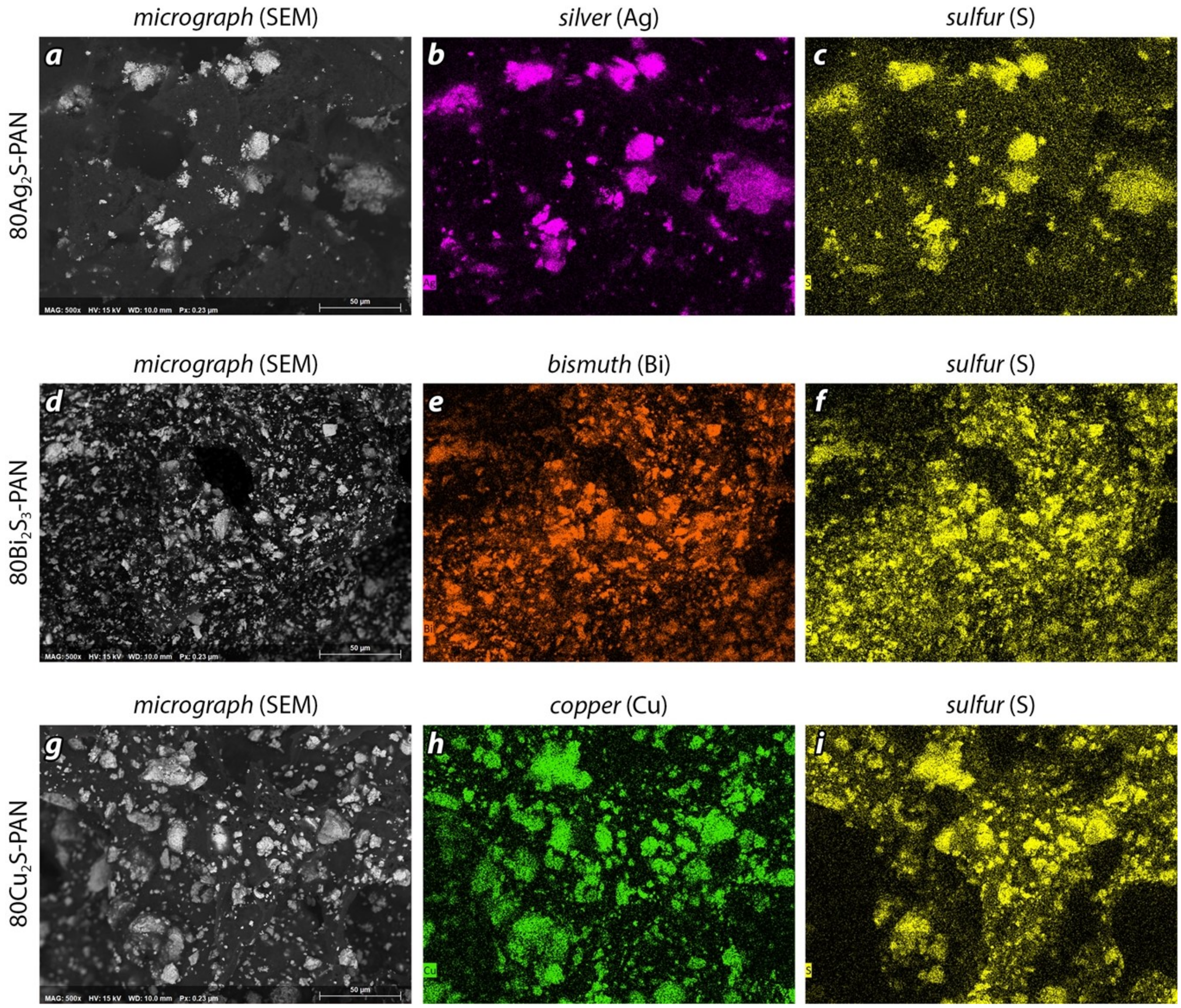

Figure S10. (a,d,g) SEM and (b,c,e,f,h,i) EDS data for (a-c) 80Ag$_2$S-PAN, (d-f) 80Bi$_2$S$_3$-PAN, and (g-i) 80Cu$_2$S-PAN composites showing the (b) Ag-map, (e) Bi-map, (h) Cu-map, and (c,f,i) S-maps.

5 Comparison with other PAN Composites for Iodine Capture

A summary of some previous experiments on PAN composites for iodine capture are provided in Table S5.

Table S5. Summary of iodine loading in PAN composites from the literature including the composite sorbent type, the active sorbent, the loading temperature (T_{LOAD}), the iodine loading (q_e = mg/g), and the reference.

Sorbent type	Sorbent (mass%)	T_{LOAD} (°C)	Iodine loading (mg/g)	Reference
75Ag-PAN	Ag^0 (75%)	120	753	Chong et al.[S1]
75Bi-PAN	Bi^0 (75%)	120	474	Chong et al.[S1]
75Cu-PAN	Cu^0 (75%)	120	1457	Chong et al.[S1]
75Sn-PAN	Sn^0 (75%)	120	1669	Chong et al.[S1]
$x$$Bi_2S_3$-PAN	Bi_2S_3 (30, 50, 70, 80, 90%)	85	490–1203	Yu et al.[S5]
$x$$SnS_2$-PAN	SnS_2 (10, 30, 50, 70, 80, 90%)	85	536–2727	Yu et al.[S6]
$x$$Sn_2S_3$-PAN	Sn_2S_3 chalcogel (33, 50%)	20–25	487, 1144	Riley et al.[S4]
75Ag_2S-PAN	Ag_2S (75%)	130	668	*Current study*
80Ag_2S-PAN	Ag_2S (80%)	130	723	*Current study*
90Ag_2S-PAN	Ag_2S (90%)	130	826	*Current study*
80Bi_2S_3-PAN	Bi_2S_3 (80%)	130	909	*Current study*
80Cu_2S-PAN	Cu_2S (80%)	130	1095	*Current study*

6 References

S1. S. Chong, B. J. Riley, R. M. Asmussen, A. Fujii Yamagata, J. Marcial, S. Lee and C. A. Burns, *ACS Appl. Polym. Mater.*, 2022, **4**, 9040-9051.
S2. B. J. Riley, S. Chong and C. L. Beck, *Ind. Eng. Chem. Res.*, 2021, **60**, 17162-17173.
S3. B. J. Riley, S. Chong, R. M. Asmussen, A. Bourchy and M. H. Engelhard, *ACS Appl. Polym. Mater.*, 2021, **3**, 3344-3353.
S4. B. J. Riley, D. Pierce, A, J. Chun, J. Matyáš, W. C. Lepry, T. Garn, J. Law and M. G. Kanatzidis, *Environ. Sci. Technol.*, 2014, **48**, 5832-5839.
S5. Q. Yu, X. Jiang, Z. Cheng, Y. Liao, Q. Pu and M. Duan, *New J. Chem.*, 2020, **44**, 16759-16768.
S6. Q. Yu, X. Jiang and M. Duan, *Soc. Sci. Res. Net.*, 2021, DOI: 10.2139/ssrn.3978461.